Multi-objective optimization design of the transmission system parameters of a dual-motor-driven electric tractor based on improved deep deterministic policy gradient algorithm

Wenxiang Xu[1], Yejun Zhu[1*], Yonggang Zhang[2,4], Maohua Xiao[1*], Liyou Xu[2,3*], Wenbo Wei[1], Hongxiang Wang[5]

(1. *College of Engineering, Nanjing Agricultural University, Nanjing 210031, China*;
2. *College of Vehicle and Traffic Engineering, Henan University of Science and Technology, Luoyang 471003, Henan, China*;
3. *State Key Laboratory of Intelligent Agricultural Power Equipment, Luoyang 471039, Henan, China*;
4. *Yisu Information Technologies Co., Ltd., Shanghai 201100, China*;
5. *Jiangsu Electronic Information Vocational College, Huai'an 223003, China*)

Abstract: Electric tractors driven by dual motors have become a critical research topic in the field of pure electric tractor research. As a key component of the transmission system, the optimization of the internal parameters of the power-coupled transmission gearbox has a crucial impact on the power transmission of the whole machine. This work combines the characteristics of low speed and high torque during tractor operation, and adopts the transmission form of double motor input and double planetary group coupling output to design the transmission structure of the gearbox. Then, this paper proposes a dynamic optimization method of the transmission system based on the Improved Deep Deterministic Policy Gradient (IDDPG) algorithm, which realizes the optimization of the gear ratio of the transmission system by constructing a virtual prototype and hardware-in-the-loop simulation environment. In transport mode, the optimized gear ratios shorten the acceleration time of the tractor from 0-20 km/h by 13.6% and increase the motor efficiency by 10%; in rotary mode, the acceleration performance is improved by 28.5% and the motor efficiency is increased by 5%. The study shows that the proposed method is significantly better than the traditional static design and provides a new technical path for the intelligent optimization of the electric tractor drive train, while promoting the efficient and sustainable development of agricultural machinery.

Keywords: electric tractors, transmission system, parameter optimization, optimization algorithm, gear ratios
DOI: 10.25165/j.ijabe.20251802.8978

Citation: Xu W X, Zhu Y J, Zhang Y G, Xiao M H, Xu L Y, Wei W B, et al. Multi-objective optimization design of the transmission system parameters of a dual-motor-driven electric tractor based on improved deep deterministic policy gradient algorithm. Int J Agric & Biol Eng, 2025; 18(2): 100–114.

1 Introduction

The rapid advancement and prosperity of humanity depend on the continuous progress of agriculture. Precision control of agricultural equipment and low-emission agricultural machinery have played an important role in meeting human demands on the natural environment[1,2]. Tractors play a pivotal role in the realm of agricultural machinery, particularly in promoting agricultural modernization and sustainable development. Pure electric tractors have attracted significant attention in agricultural machinery due to the growing emphasis on these aspects. Electric tractors offer a multitude of advantages, including enhanced controllability, heightened precision, and zero energy terminal emissions. Moreover, the operation of these tractors results in minimal environmental pollution, thereby contributing to the reduction of agricultural production's reliance on fossil fuels[3,4]. Given these distinctive features, electric tractors hold immense potential for application in precision agriculture.

In recent years, significant progress has been achieved in the research and development of electric tractors, primarily driven by advancements in battery technology and the declining prices of battery packs. Accordingly, the conversion of diesel tractors into electric tractors has emerged as a cost-effective solution[5]. This situation has led to a rapid expansion in the field of electric tractor research and development over the past decade. Electric tractors can be classified into two categories based on the number of electric motors: single-motor-driven and dual-motor-driven tractors. Some studies have extensively explored the single-motor-driven tractor. Chen et al.[6] presented an energy management strategy design based on optimization techniques. This design optimally adjusts the power distribution among various energy sources and the motor, thereby enhancing the overall efficiency and economy of the tractor. Xu et al.[7] presented an energy management strategy design based on optimization techniques. This design optimally adjusts the power

Received date: 2024-04-02 **Accepted date:** 2024-12-12
Biographies: Wenxiang Xu, PhD candidate, research interest: cooperative control of distributed electric drive systems for agricultural machinery, Email: xu18561264629@163.com; **Yonggang Zhang**, MS, research interest: drive train for electric farm machinery, Email: pzhang994@gmail.com; **Wenbo Wei**, PhD candidate, research interest: multi-machine collaboration of agricultural equipment, Email: wboclear@stu.njau.edu.cn; **Hongxiang Wang**, PhD, Associate Professor, research interest: intelligent agricultural machinery, Email: 651108384@qq.com.
***Corresponding author: Yejun Zhu**, PhD, Lecturer, research interest: intelligent agricultural machinery, Email: yjzhu@njau.edu.cn; **Maohua Xiao**, Professor, research interest: intelligent agricultural machinery. Nanjing Agricultural University, No.666 Binjiang Road, Nanjing 210031, China. Tel: +86-13951756153, Email: xiaomaohua@njau.edu.cn; **Liyou Xu**, Professor, research interest: vehicle transmission theory and control technology. Henan University of Science and Technology, No.48 Xiyuan Road, Luoyang 471000, Henan, China. Tel: +86-13663873262, Email: xlyou@haust.edu.cn.

distribution among various energy sources and the motor, thereby enhancing the overall efficiency and economy of the tractor. Tomasikova et al.[8] conducted extensive modeling, simulation, and analysis of the electromechanical system, focusing on the physical characteristics of the vehicle. Furthermore, a modular simulation and design platform for single-motor drive systems was developed. The dual-motor coupled transmission system has emerged as a prominent transmission scheme for electric tractors due to advancements in motor technology and power supply systems. This system has gained recognition as a mainstream solution through continuous demonstration and development. Xie et al.[9] introduced a novel electric tractor drive system featuring dual electric motors and a coupled transmission system. A prototype was fabricated, and the simulation results demonstrated an efficiency improvement rate of 9.92% and 12.36% in plowing and wheeling, respectively. Wen et al.[10-14] proposed a dual-motor single-shaft powertrain structure that enhances power performance and system stability through the cooperative operation of the two electric motors. The sub-motor remains coupled with the drive train, resulting in a simple structure conducive to the development of sub-motor braking energy recovery control. In summary, the continuous demonstration and development of the dual-motor coupled transmission system have established it as a mainstream solution for electric tractors. This work lays a solid foundation for the future development of electric tractor transmission systems.

The transmission system plays a critical role in electric tractors, as the rational design of its parameters greatly influences the traction performance and overall economy[15-18]. Extensive research has been conducted by numerous scholars on electric tractor transmission systems, resulting in significant advancements in enhancing the vehicle's strength and economy. Wang et al.[19] introduced a novel control system for electric tractors equipped with a dual-motor coupled drive. The system combined a demand torque calculation method, a drive torque allocation strategy based on nonlinear PID control, and an improved serpentine optimizer algorithm. This integrated approach resulted in significant improvements in the efficiency and stability of the drive train. Regazzi et al.[20] conducted numerical simulations to investigate the influence of various tractor design parameters on power delivery efficiency. The key design parameters were identified by quantifying their effects on traction performance, resulting in the establishment of a quantitative relational equation for optimizing the optimal mass distribution. Xia et al.[21] proposed a multi-objective optimal design numerical model for tractor transmission by using the NSGA-II multi-objective genetic algorithm to achieve optimization. Chen et al.[22] developed an auto-start control strategy for tractors paired with a new powershift transmission. The strategy effectively prevented transmission failure caused by elevated temperature and excessive contact friction[23]. Molari et al.[24] evaluated the working conditions of high-horsepower tractors to identify the causes of energy loss and analyzed the transmission start-up situation and power absorbed by each gear. Choi et al.[25] utilized a genetic algorithm to optimize tractor transmission gear whistling noise, resulting in improved static transmission stability of the system. Ouyang et al.[26] proposed a shift law strategy based on a robust tracking control algorithm to achieve precise control and fast response of the shift actuator. The effectiveness of the proposed controller was verified through experimental evaluation.

Electric tractors primarily operate in low rotational speed and high torque conditions, frequently encountering resistance fluctuations during plowing operations[27,28]. A small gearbox is commonly adopted to regulate different modes of tractor transportation and plowing to mitigate the motor's load shocks. Extensive research has demonstrated that optimization of the gearbox can yield significant improvements in energy efficiency, gas emission reduction, and overall vehicle performance[29-32]. Once the structure of the transmission system and the power selection parameters are finalized, the careful selection of gear ratios becomes crucial in determining the performance of the tractor[33-36]. In summary, current research efforts primarily focus on the powertrain configuration and body structure design of electric tractors. The transmission system arrangement, which uses dual motor power input and dual planetary row coupling power output, has advanced to a greater level of maturity. However, the optimization of transmission system parameters for electric tractors remains relatively limited. Therefore, a suitable method for optimizing the transmission system gearbox parameters must be utilized.

This study focuses on the transmission system of electric tractors, specifically those equipped with dual motor power input and dual planetary row coupling power output, to address the aforementioned challenges. The aim is to optimize the transmission speed ratios of each gear using the IDDPG algorithm coupled with a virtual prototype technology for dynamic parameter optimization. Initially, the electric tractor's transmission system model is constructed using Simscape and integrated into the tractor simulation environment to establish a comprehensive simulation model. Subsequently, the dynamic optimization model for the transmission system parameters is formulated, utilizing the DDPG strategy. The objective parameters considered are the minimum coupled total transmission ratio, the shortest acceleration time, and the highest motor efficiency. By contrast, the optimization parameters are the transmission speed ratios of each gear. The transport mode and rotary tillage mode conditions are selected for analysis to validate the effectiveness of the proposed dynamic optimization approach. The dynamic optimization model of the transmission system parameters is then jointly simulated with the entire machine model using hardware-in-the-loop technology. A comparative analysis is performed, comparing the results with the target parameters obtained from static design, thereby confirming the superior performance of the dynamic optimization strategy proposed in this study. The specific study structure flow chart is shown in Figure 1.

2 Dual-motor coupled-drive electric tractor model

In this chapter, the structure of the electric tractor transmission is analyzed, and the main parameters of the power coupling device are determined using traditional static calculations. A CAD model of the transmission system is developed and imported into Simscape to construct a physical domain model. A comprehensive simulation environment, incorporating the tractor body, driver, and dual-motor models, is established to analyze the performance of the dual-motor coupled transmission. The physical domain driveline model is seamlessly integrated into this environment, enabling the development of a virtual prototype. This prototype facilitates simulations and evaluations, providing insights into the overall performance and functionality of the electric tractor transmission system.

2.1 Study of the structure of the transmission system

After extensive research, the dual-motor-driven electric tractor power drive has evolved into a mature program for the structural arrangement of electric tractors. This program primarily relies on the dual-motor power input and planetary row coupling output,

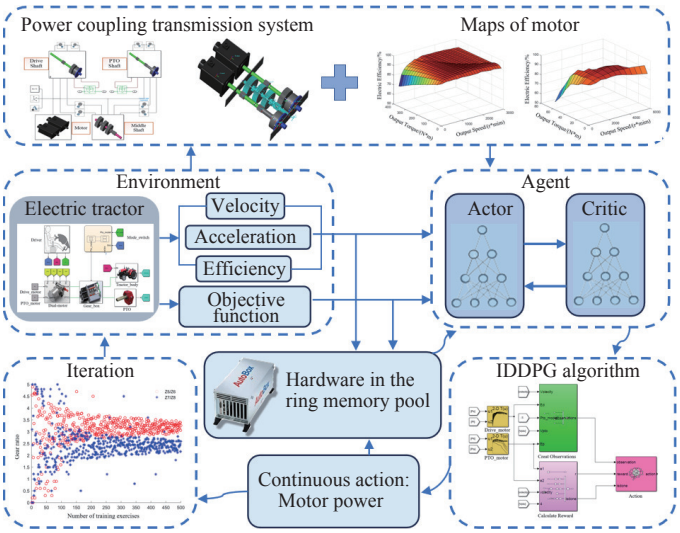

Figure 1 Research structure flow chart

giving rise to various transmission structures. The structure exemplified by the multi-planet row coupling drive system holds significant value in the investigation of transmission systems for electric tractors propelled by two motors[10]. In this study, we examine a dual motor power input and dual planetary row coupling output transmission system as the focal point of our investigation.

The transmission system structure (Figure 2) transfers motor power to the input shaft, driving the sun wheel while locking the gear ring. Power is output through the planetary carrier to the drive shaft. The drive and PTO motors can operate independently. Under substantial PTO load, the drive motor transmits power to the PTO shaft via the intermediate shaft, while under heavy drive shaft load, the PTO motor supplies power to the drive shaft. The driving force is transmitted to the rear axle through the main gearbox. The system includes two synchronizers and two brakes, enabling four power transmission routes for transport and rotary modes. In independent drive mode, with synchronizers 1 and 2 disengaged, the motors decouple and independently output power through planetary mechanisms 4 and 5.

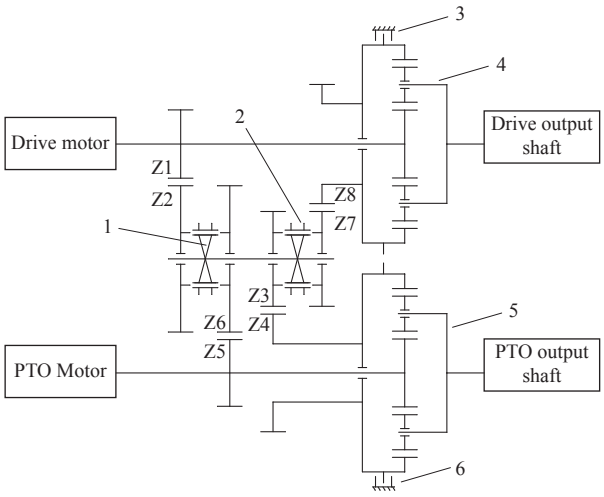

Figure 2 Structure schematic of the dual motor power input and dual planetary row coupling output transmission system

In the transport mode, the tractor operates with synchronizers 1 and 2 engaged to the right. During this state, the power supplied by the PTO motor passes through the transmission gear pair Z5Z6 and Z7Z8 within the planetary gear mechanism 4. The power is then combined and outputted alongside the power provided by the drive motor.

In the rotary plowing mode, the tractor functions with synchronizers 1 and 2 simultaneously engaged to the left. In this mode, the power provided by the drive motor is transmitted through the transmission gear pair Z1Z2 and Z3Z4 within the planetary gear mechanism 5. The power is then coupled with the power supplied by the PTO motor.

These configurations enable the tractor to efficiently transition between the transport and rotary modes, utilizing the appropriate power sources and transmission gear mechanisms. The corresponding controller is switched based on the various working modes of the tractor, and the power coupling mode is adjusted accordingly. Table 1 summarizes the status of each component under different working modes, showing how synchronizers and brakes adjust the power flow.

Table 1 Status of each component under different conditions

Mode	Drive motor	PTO motor	Synchronizer 1	Synchronizer 2	Brake 1	Brake 2
Park	○	○	○	○	●	●
Low speed (transport)	●	○	○	○	●	○
High speed (transport)	●	●	→	→	○	○
Low load (rotary plowing)	●	●	○	○	●	●
High load (rotary plowing)	●	●	←	←	●	○
Reverse	●	○	○	○	●	○

2.2 Traditional static design of the main parameters of the transmission system

The gear ratio, as a critical parameter of the transmission system, exerts a significant influence on its performance[33-36]. In conventional transmission system design, the gear ratio is typically selected after determining the system structure based on the design requirements. This process involves utilizing traditional static calculations to verify if the chosen gear ratio satisfies the design criteria. Subsequently, the static design of the other parameters in the power coupling device of the transmission system, such as the number of teeth of the meshing gears, module, and pressure angle, will be accomplished.

Several studies in the literature have discussed the methodology for conducting static calculations in gear design[37-39]. A gear module g is designed according to the bending fatigue strength of the tooth

root to simultaneously meet the bending and contact fatigue strength:

$$m_{nt} \geq \sqrt[3]{\frac{2k_{Ft}T_1Y_\varepsilon Y_\beta \cos^2\beta}{\phi_d z_a^2} \cdot \left(\frac{Y_{Fa}Y_{sa}}{[\sigma_F]}\right)} \quad (1)$$

$$m_n = m_{nt}\sqrt[3]{\frac{K_F}{K_{Ft}}} \quad (2)$$

where, m_{nt} is the modulus of the trial gear; k_{Ft} is the trial load coefficient; T_1 is the transmission torque of the active gear, N·m; Y_ε is the overlap coefficient; Y_β is the helix angle coefficient; β is the initial helix angle, (°); ϕ_d is the tooth width coefficient; z_a is the number of teeth of the active gear; Y_{Fa} is the tooth shape coefficient; Y_{sa} is the stress correction coefficient; σ_F is the bending fatigue permissible stress, Pa; and K_F is the load coefficient.

The indexing circle diameter d1 is designed according to the contact fatigue strength of the tooth surface as follows:

$$d_{1t} \geq \sqrt[3]{\frac{2K_{Ht}T_1}{\phi_d} \cdot \frac{u+1}{u} \cdot \left(\frac{Z_H Z_E Z_\varepsilon Z_\beta}{[\sigma_H]}\right)^2} \quad (3)$$

$$d_1 = d_{1t}\sqrt[3]{\frac{K_H}{K_{Ht}}} \quad (4)$$

where, d_{1t} is the trial indexing circle diameter, m; K_{Ht} is the trial load coefficient; u is the transmission ratio; Z_H is the area coefficient; Z_E is the elastic influence coefficient; Z_ε is the overlap coefficient; Z_β is the helix angle coefficient; and σ_H is the contact fatigue allowable stress, Pa.

Statics, as a branch of theoretical mechanics, investigates the laws of equilibrium within a system of masses subjected to external forces. This aspect also encompasses the application of relativistic generalized equilibrium equations to rotating systems and their relevance to driveline system design. Consequently, statics serves as a fundamental approach to analyzing force systems and the forces acting on objects, enabling the design of driveline shaft cross-sections[40,41]. Initially, equilibrium conditions are utilized to solve for the unknown restraining forces caused by specified loads on the shaft. Subsequently, the strength and stiffness of the shaft are assessed through analysis.

$$P = P_0 + \rho g h = P_0 + Yh \quad (5)$$

where, P is the pressure at any point, Pa; P_0 is the surface pressure, Pa; Y is weight per unit volume of liquid, N/m³; ρ is the density, kg/m³; g is the acceleration of gravity, m/s²; h is the height of the liquid, m.

We derived the gear parameter configuration table through hydrostatic calculation by utilizing the aforementioned calculation method and taking into account the parameters of the Dongfanghong 1804 model tractor from China YTO Group. This configuration table was developed based on the operational requirements of the tractor, in conjunction with Figure 2. Table 2 lists the transmission system gear parameters obtained by traditional static calculation.

Table 2 Gear parameters for the dual-motor transmission system

Parameter term	Tooth number z	Modulus m	Pressure angle α/(°)	Helix angle β/(°)	Tooth width b/mm
Gear pair 1/2	31/99	3	20	14.12	96/92
Gear pair 3/4	29/93	3	20	13.79	86/90
Gear pair 5/6	29/93	3	20	13.79	90/86
Gear pair 7/8	31/99	3	20	14.12	96/92
Sun gear 4	25	4	20	14	76
Planet gear 4	19	4	20	14	76
Gear ring 4	62	4	20	14	76
Sun gear 5	25	4	20	14	76
Planet gear 5	19	4	20	14	76
Gear ring 5	62	4	20	14	76

2.3 Transmission system modeling

2.3.1 CAD modeling of the transmission system

After the transmission system parameters have been determined, a 3D parametric model of the power coupling mechanism is constructed using SolidWorks software based on the mathematical model of the transmission system. The specific parameters are instantiated within the model. Figure 3 illustrates the 3D model of the electric tractor's dual-motor coupled transmission system structure, incorporating the drive and PTO motors connected to the front of the transmission. The main input and sub-input shafts are linked to the transmission housing on one end, while the other end is connected to the sun wheel of the planetary carrier. Therefore, the planetary carrier serves as the power output element, transmitting power to the main gearbox and the PTO shaft.

2.3.2 Simulation modeling of the transmission system

The CAD interpretation file is generated using the Simscape Multibody Link plug-in to facilitate the construction of the drive train model in the physical domain. Subsequently, the CAD file is imported into Simulink using MATLAB to construct the transmission system simulation model (Figure 4).

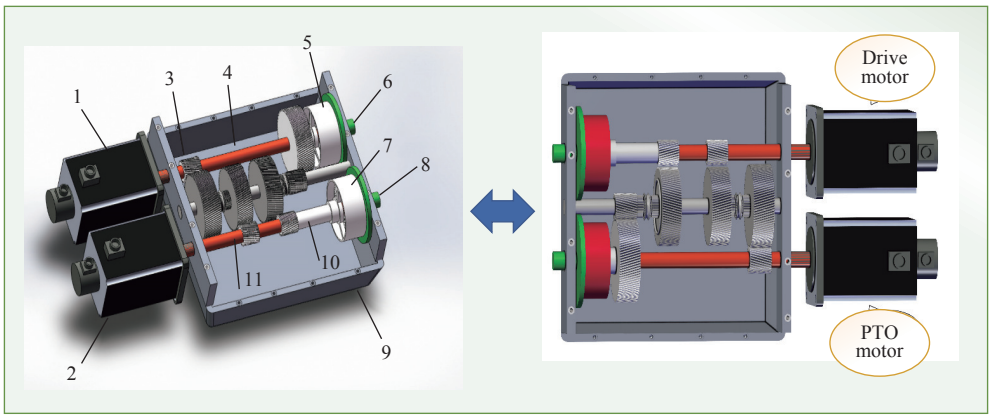

1. Drive motor 2. PTO motor 3. Gear 1 4. Main drive shaft 5. Main drive shaft planetary mechanism 6. Drive output shaft 7. Secondary drive shaft planetary mechanism 8. PTO output shaft 9. Gearbox housing 10. Ring sleeve 11. Secondary drive shaft

Figure 3 3D CAD model of the electric tractor transmission system

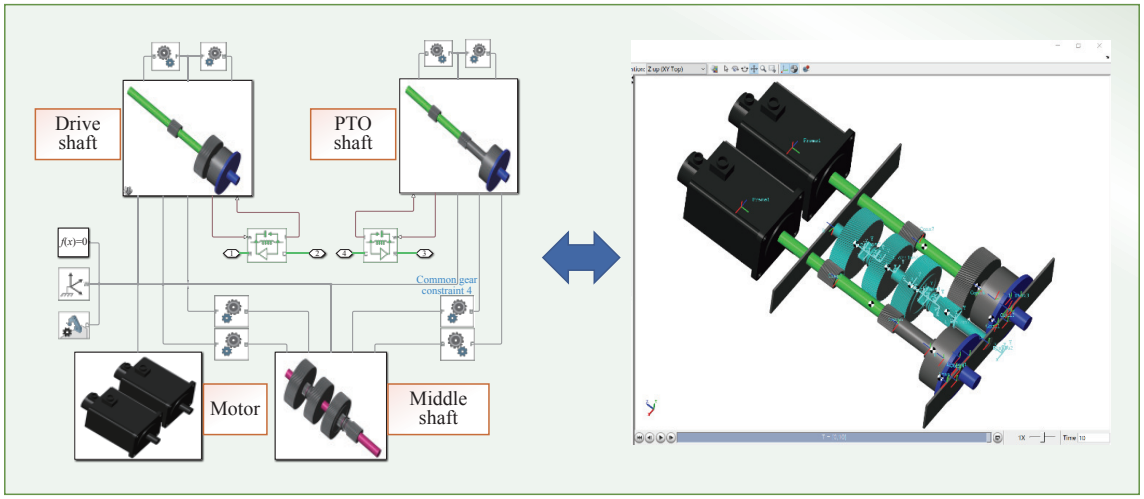

Figure 4 Simscape physical domain simulation model of the electric tractor transmission system

2.4 Transmission system modeling

2.4.1 Driver model

The driver model serves as a predictive drive module, functioning akin to a controller. This model generates normalized steering, acceleration, and braking commands to track longitudinal velocity and lateral reference displacement[42,43]. In this work, the monorail model is utilized for optimal single-point preview control. The external actions parameter is utilized to create input ports for the signals, and a PI control method is selected for longitudinal control. The modeling techniques associated with this topic are well-established and straightforward. Therefore, this work will not extensively delve into the modeling details[44-46].

2.4.2 Motor model

The permanent magnet synchronous motor finds wide-ranging applications in the electric vehicle industry due to its high efficiency, superior performance, and precise control capabilities. This motor is commonly employed across various sectors, such as industry and transportation. The motor's construction principle is illustrated in Figure 5. A rotating magnetic field with a sinusoidal rate of change is generated based on the rotor angle by utilizing permanent magnets. The rotor angle is defined as the angle between the a-phase magnetic axis and the d-axis or q-axis. When the rotor mechanical angle θ_r is zero, the a-phase and permanent magnet fluxes align.

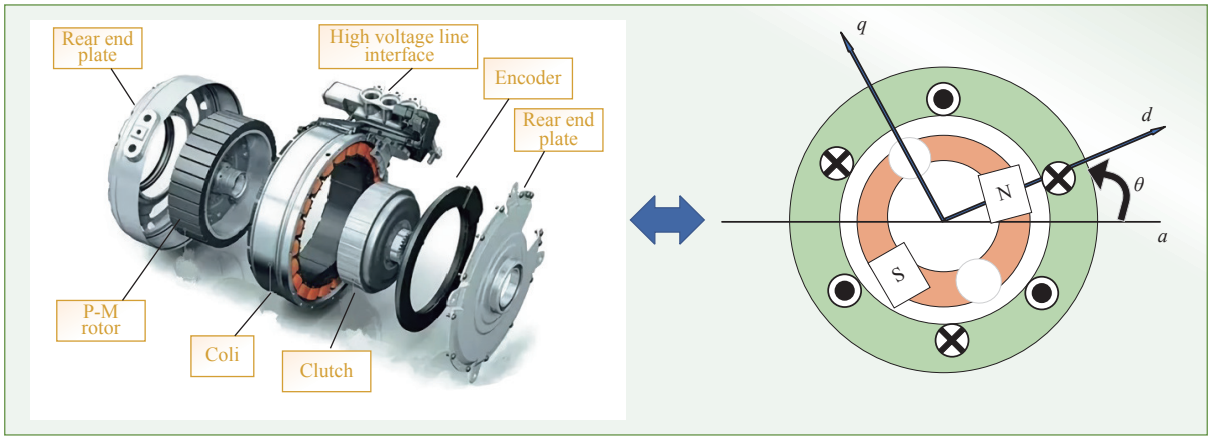

Figure 5 Simscape physical domain simulation model of the electric tractor transmission system

The voltage of the stator winding is determined as follows:

$$\begin{bmatrix} v_a \\ v_b \\ v_c \end{bmatrix} = \begin{bmatrix} R_s & 0 & 0 \\ 0 & R_s & 0 \\ 0 & 0 & R_s \end{bmatrix} \begin{bmatrix} i_a \\ i_b \\ i_c \end{bmatrix} + \begin{bmatrix} \frac{d\psi_a}{dt} \\ \frac{d\psi_b}{dt} \\ \frac{d\psi_c}{dt} \end{bmatrix} \quad (6)$$

where, v_a, v_b, and v_c are the individual phase voltages across the stator windings; R_s is the equivalent resistance of each stator winding; i_a, i_b, and i_c are the currents flowing through the stator windings; and $\frac{d\psi_a}{dt}$, $\frac{d\psi_b}{dt}$, and $\frac{d\psi_c}{dt}$ are the rate of change of the magnetic flux in each stator winding.

The permanent magnets and the three-phase windings constitute the total flux connected to each winding. The total flux is determined as follows:

$$\begin{bmatrix} y_a \\ y_b \\ y_c \end{bmatrix} = \begin{bmatrix} L_{aa} & L_{ab} & L_{ac} \\ L_{ba} & L_{bb} & L_{bc} \\ L_{ca} & L_{cb} & L_{cc} \end{bmatrix} \begin{bmatrix} i_a \\ i_b \\ i_c \end{bmatrix} + \begin{bmatrix} y_{am} \\ y_{bm} \\ y_{cm} \end{bmatrix} \quad (7)$$

where, ψ_a, ψ_b, and ψ_c are the total magnetic flux connecting each stator winding; L_{aa}, L_{bb}, and L_{cc} are the self-inductance coefficients of stator windings; L_{ab}, L_{ac}, and L_{ba} are the transmission structure of dual motormagnet fluxes connecting the stator windings.

The power system investigated in this work for the electric tractor incorporates two permanent magnet synchronous motors. The appropriate motor models are selected based on the working demands of the tractor to optimize power utilization and minimize wastage due to excess power. The main parameters of the drive and PTO motors are determined by conducting a power matching analysis considering the power demand of the Dongfanghong 1804 model tractor (Table 3).

Table 3 Main motor specifications for the electric tractor

Parameter	Value
Rated voltage of the drive motor/V	100
Rated power of the drive motor/kW	90
Rated torque of the drive motor/N·m	1140
Rated speed of the PTO motor/r·min^{-1}	760
Maximum speed of the PTO motor/r·min^{-1}	3000
Rated voltage of the PTO motor/V	110
Rated power of the PTO motor/kW	48
Rated torque of the PTO motor/N·m	230
Rated speed of the PTO motor/r·min^{-1}	2000
Maximum speed of the PTO motor/r·min^{-1}	6000

A power system test rig was constructed to acquire the motor efficiency model for the chosen motor type[47]. Bench tests were conducted to measure the rotational speed, torque, bus voltage, and current. Figure 6 illustrates the power system test rig used in the experiments.

The motor efficiency is calculated as follows:

$$\eta = \frac{P_{\text{out}}}{P_{\text{in}}} = \frac{T_m n_m}{UI} \times 100\% \tag{8}$$

where, η is the motor output efficiency, %; P_{out} is the motor output power, W; P_{in} is the motor input power, W; U is the bus voltage, V; I is the bus current, A; T_m is the motor torque, N·m; and n_m is the motor speed, r/min.

The motor's efficiency at various rotational speeds and torques was experimentally calculated, and the obtained discrete data points were fitted using interpolation techniques to generate the motor's efficiency map. Figure 7 illustrates the efficiency maps of the drive and PTO motors.

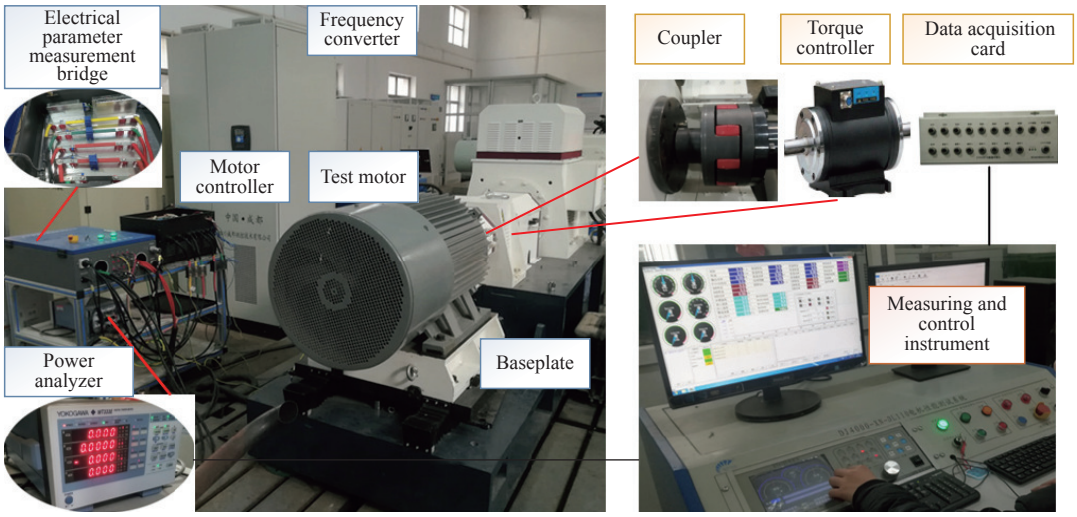

Figure 6 Power system test platform

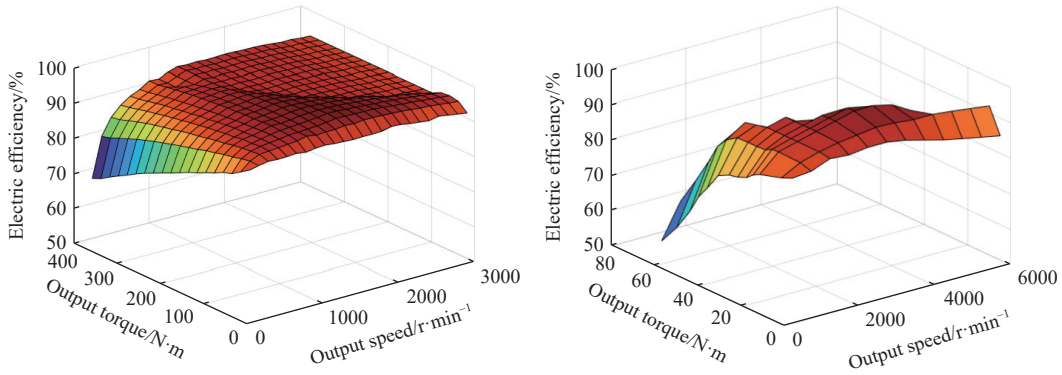

a. Efficiency map of the drive motor b. Efficiency map of the PTO motor

Figure 7 Efficiency map of the motors

The results indicate that the drive motor exhibits an efficiency exceeding 90% within the operating range of 550-900 r/min during the transportation mode. Correspondingly, this speed range translates to a vehicle speed of 0-27.76 km/h. In the PTO motor-assisted mode, the corresponding speed range extends from 10 to 38.14 km/h. These findings demonstrate that the motor system is capable of meeting a broad spectrum of operational requirements, encompassing transportation and rotary plowing tasks.

The dual motor model receives control signals from the driver model and delivers rotational power to the transmission system. Experimental motor data are utilized to generate a lookup table, which enables the creation of a motor simulation model. This simulation model ensures quick and accurate response when torque and speed demands are applied to the motor.

2.4.3 Virtual prototype simulation environment for electric tractors

The electric tractor model comprises a six-degree-of-freedom body model with a front axle featuring transverse swinging degrees of freedom, along with four rotatable wheels. Ackermann steering equations are utilized to control the steering of the front wheels[48]. The simulation results are utilized to plot the forces and torques at the contact patches, enabling visualization and analysis of the simulation outcomes. The electric tractor is configured with rear-

wheel drive, and air resistance is disregarded for modeling. Given that the tractor predominantly experiences longitudinal forces during its operation, the modeling process solely focuses on considering the longitudinal force to construct the parametric model of the tractor[49]. The simulation environment model of the virtual prototype for the electric tractor is established by collecting signals from the driver's accelerator pedal, brake pedal, and PTO manipulation switch. The working mode switching is implemented using Stateflow. Figure 8 illustrates the virtual prototype's simulation environment model.

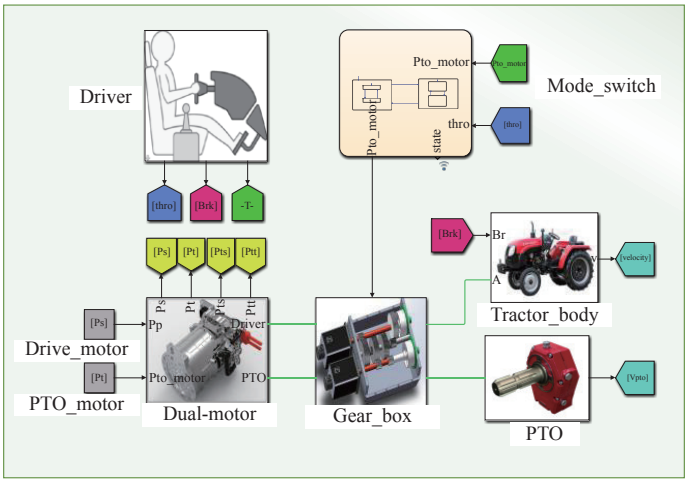

Figure 8 Electric tractor simulation environment model

The simulation environment comprises the driver model, two-motor model, drive train model, tractor model, and mode-switching model. The driver model generates control signals for the accelerator, brake, and PTO, with the PTO signal (1×2 dimensional) indicating switching states and working modes (fixed-speed or follower) based on predefined conditions (Table 1). The dual-motor model processes these signals to output motor speed and torque, which are coupled in the drive train model to provide driving and PTO power outputs. The tractor model converts driving force into vehicle speed signals. Together, these components form the virtual prototype of the dual-motor coupled transmission system, serving as the foundation for parameter optimization.

3 Optimal design of the transmission system parameters based on IDDPG

Optimization of the drive train parameters by using a suitable optimization algorithm to maximize the reward function is a significant approach in general scientific research. In this chapter, an enhanced version of the deep deterministic policy gradient (DDPG) algorithm is proposed to mitigate the influence of fixed coupling laws resulting from different transmission ratios. The objective function is formulated to include three key factors: minimizing the overall transmission ratio, achieving the shortest acceleration time, and maximizing motor efficiency. The optimization parameter used is the transmission speed ratio of each gear, which is adjusted to align with the motor coupling law.

3.1 DDPG algorithm model

The DDPG algorithm is a model-free, online, off-policy reinforcement learning method. A DDPG agent is an actor-critic reinforcement learning agent that searches for an optimal policy that maximizes the expected cumulative long-term reward. The DDPG algorithm utilizes deep neural networks, specifically two: the critic network and the actor network. Both networks are constructed, and the actor and critic models are updated in each step. The DDPG agent discovers the optimal strategy by utilizing the actor-critic reinforcement learning method and ultimately achieves the highest reward accumulation[50]. The flow and model configuration of the DDPG algorithm are depicted in Figure 9.

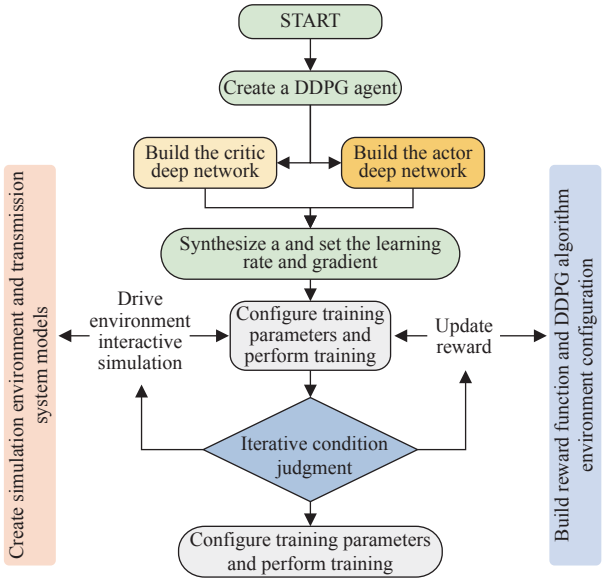

Figure 9 Flowchart of the DDPG algorithm

critic $Q(S,A;\phi)$ is initialized with random parameter value ϕ; target *critic* is initialized with target critic parameter ϕ_t, thus $\phi_t=\phi$; *actor* $\pi(S)$ is initialized with random parameter value θ; and *actor* is initialized with parameter θ_t, thus $\theta_t=\theta$. In the current observation S, action A is chosen as follows:

$$A=\pi(S)+N \tag{9}$$

where, N is stochastic noise from the noise model.

Action A is executed, and the reward value R and the next observation S' are observed. $(S\ A\ R\ S')$ is stored in the experience buffer. If S_i' is the termination state, then the value function target y_i is set to R_i, otherwise:

$$y_i=R_i+\gamma Q_t(S_i',p_t(S_i';Q_t);f_t). \tag{10}$$

The objective value of the function is the sum of the execution reward value R_i and the future discount to the current reward. γ is the discount factor. To calculate the cumulative reward, the agent takes the following observation S_i' from the sampled experience and

passes it to the target action function to compute the subsequent action. The cumulative reward is then obtained by forwarding the next action to the target *critic*.

The critic parameters are updated by minimizing the loss L across all sampled experiences:

$$L = \frac{1}{2M}\sum_{i=1}^{M}(y_i - Q(S_i, A_i; \phi))^2 \tag{11}$$

The actor parameters are updated by using the following sampled policy gradient to maximize the expected discounted reward:

$$\begin{cases} \nabla_\theta J \approx \dfrac{1}{M}\sum_{i=1}^{M} G_{ai} G_{\pi i} \\ G_{ai} = \nabla_A Q(S_i, A|\theta) \\ A = \pi(S_i|\theta) \\ G_{\pi i} = \nabla_\theta \pi(S_i|\theta) \end{cases} \tag{12}$$

where, G_{ai} is the gradient of the critic output with respect to the action computed by the actor network; and $G_{\pi i}$ is the gradient of the actor output with respect to the actor parameters. Both gradients are evaluated for observation S_i.

In the construction of the reward function, we choose motor efficiency and transmission ratio as the main optimization indicators, mainly for the following reasons:

Motor efficiency: Motor efficiency directly reflects the utilization of electricity and is an important indicator for the optimization of energy consumption of electric tractors. High efficiency means that a unit of electrical energy can be converted into more mechanical energy, thus reducing power waste and improving range; improved motor efficiency also reduces heat dissipation and energy loss, thus extending equipment life and reducing operation and maintenance costs.

Transmission ratio: The transmission ratio is a key parameter affecting the tractor's acceleration and load adaptability. Optimizing the transmission ratio can ensure that the tractor achieves the best power distribution under different working conditions (such as transport mode and rotary mode); the reasonable design of the transmission ratio can also reduce the shock load and improve the stability and reliability of the system operation.

The efficiency of the drive motor, the efficiency of the PTO motor, the target vehicle speed following error, and the total transmission ratio are used in the reward function, which is constructed from four parameters:

$$\gamma = -(0.1E_d + 0.1E_P + 0.3E_s + 0.05^2) + 100B \tag{13}$$

where, E_d is the drive motor efficiency, E_P is the PTO motor efficiency, E_s is the difference between the actual speed and the target speed, and B is the action space boundary value.

The reward function combines two core metrics, motor efficiency and transmission ratio, and aims to strike a balance between the following objectives: maximizing the motor efficiency to optimize the energy utilization of the tractor for a given operating condition; optimizing the transmission ratio to reduce unnecessary energy wastage, while improving the stability and responsiveness of the system; and minimizing the acceleration time to ensure better dynamics of the tractor.

3.2 Improved DDPG algorithm model

Despite the popularity of DDPG as a reinforcement learning algorithm that extends the classical actor-critic approach to continuous action spaces, it still exhibits several limitations and common drawbacks, which are outlined as follows:

(1) High computational complexity: DDPG involves numerous neural network updates, resulting in significant computational overhead, particularly in complex environments or with large action spaces.

(2) Vulnerability to overfitting: DDPG may overfit to specific environments and exhibit limited generalization capabilities to novel environments or scenarios. Consequently, performance can suffer, and learning can be slow.

(3) Difficulty with high-dimensional state spaces: DDPG encounters challenges when handling high-dimensional state spaces, resulting in slow learning and suboptimal strategies.

(4) Sensitivity to hyperparameters: DDPG relies on careful tuning of the hyperparameters for optimal performance. Improper selection of hyperparameters can result in unstable training and poor performance.

(5) Exploration–exploitation tradeoff: In scenarios with sparse rewards, DDPG can struggle to strike a balance between exploration and exploitation, resulting in slow learning or convergence to suboptimal strategies.

To address the aforementioned limitations, this work introduces an enhanced approach for the DDPG algorithm, aiming to improve its effectiveness in optimizing transmission system parameters. The following section outlines several enhancements made to the DDPG algorithm, specifically tailored to the optimization design of electric tractor driveline parameters:

(1) Batch normalization: Incorporating batch normalization in DDPG improves stability and convergence. Normalizing the inputs to the neural network before each layer prevents gradients from vanishing or spiking.

(2) Replay buffer prioritization: DDPG can experience slow learning due to irrelevant or redundant experiences in the replay buffer. Prioritizing experiences based on their desired learning value enhances sample efficiency.

(3) Target network updates: Periodic updates of the target network in DDPG reduce the correlation between the target and the online networks. Employing a soft update technique, gradually blending the online and target network parameters, enhances stability and convergence.

(4) Exploration strategy: In continuous action spaces, random actions may not effectively explore the space. Advanced exploration strategies, such as adding noise to the actor's strategy, improve exploration and mitigate local optima.

(5) Parameter sharing: Sharing parameters between the actor and the critic networks in DDPG reduces the number of learning parameters, enhancing sample efficiency. This task can be achieved through counterweighting or a shared encoder architecture.

(6) Hindsight experience replay (HER): HER improves the sample efficiency by creating new experiences based on the results of the intelligent agent's behavior, even if unsuccessful. This condition allows agents to learn from failed attempts and avoid local optima.

These enhancements effectively address some limitations of the original DDPG algorithm, improving its stability, sample efficiency, and exploration capabilities. The objective function is designed to minimize the total coupled transmission ratio, reduce acceleration time, and maximize motor efficiency, using the transmission speed ratio of each gear as the optimization parameter. This improved reinforcement learning algorithm not only reduces computational power consumption but also accelerates learning and exhibits stronger convergence performance.

IDDPG Algorithm

Step 1. Initialization:

Randomly initialize critic network $Q(s,a|\theta^Q)$ and actor $\mu(s|\theta^\mu)$ with weights θ^Q and θ^μ.

Initialize target networks Q' and μ' with weights $\theta^{Q'} \leftarrow \theta^Q$, $\theta^{\mu'} \leftarrow \theta^\mu$.

Initialize prioritized replay buffer R.

Step 2. For Each Episode:

Initialize a random process N for advanced action exploration.

Receive initial observation state S_1 and apply batch normalization.

Step 3. For Each Time Step:

Select action $a_t = \mu(s_t|\theta^\mu) + N_t$ using the current policy and exploration strategy.

Execute action a_t at and observe reward r_t and new state s_{t+1}.

Store transition (s_t, a_t, r_t, s_{t+1}) in R with prioritization.

Step 4. Learning:

Sample a random minibatch of N transitions (s_i, a_i, r_i, s_{i+1}) from R based on priority.

Set $y_i = r_i + \gamma Q'(s_{i+1}, \mu'(s_{i+1}|\theta^{\mu'})|\theta^{Q'})$.

Update critic by minimizing the loss: $L = \frac{1}{N}\sum_i (y_i - Q(s_i, a_i|\theta^Q))^2$

Update the actor policy using the sampled policy gradient:

$$\nabla_{\theta^\mu} J \approx \frac{1}{N}\sum_i \nabla_a Q(s,a|\theta^Q)|_{s=s_i, a=\mu(s_i)} \nabla_{\theta^\mu}\mu(s|\theta^\mu)|_{s_i}$$

For unsuccessful episodes, apply hindsight to reframe goals and store additional transitions in$R$.

Step 5. Soft Update Target Networks:

Softly update the target networks:

$$\theta^{Q'} \leftarrow \tau\theta^Q + (1-\tau)\theta^{Q'}$$

$$\theta^{\mu'} \leftarrow \tau\theta^\mu + (1-\tau)\theta^{\mu'}$$

Step 6. Repeat steps 2 to 5 for the desired number of episodes.

The IDDPG algorithm model is constructed in Simulink to establish the environment interface for algorithm training. The model includes the observer, calculate, and action modules (Figure 10).

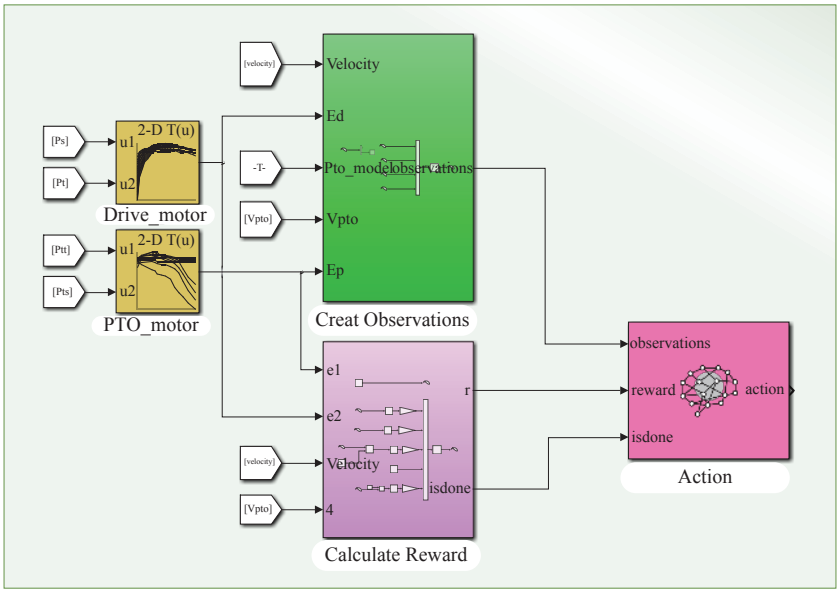

Figure 10 IDDPG algorithmic agent interface model

The agent body model consists of three input ports (observation input port, reward input port, and action execution feedback input port) and an action execution output port. An observer module and a reward calculation module are implemented to facilitate the functionalities of these input ports. The action output signals from the intelligent body are connected to a motor controller, enabling the control of the drive and PTO motors in the electric tractor. The test data for the two motors are stored in the lookup tables to optimize the efficiency. These data are directly utilized during the training of the intelligent body, resulting in time-saving benefits.

4 Joint simulation and optimization result analysis

Joint simulation analysis is an encompassing technique that combines multiple simulation methods to gain deeper insights into the behavior of complex systems. This process serves to aid researchers in promptly verifying the functionality and design flaws of engineered products, providing valuable information for decision-makers. In this chapter, we initiate the analysis by establishing the simulation working conditions. Subsequently, the IDDPG model of the transmission system parameters is co-simulated with the virtual prototype simulation environment using hardware-in-the-loop simulation technology. This process enables the attainment of theoretically optimal parameter matching for the transmission system. Finally, a comparative analysis is conducted with the static design to validate the optimization effects.

4.1 Parameter configuration of simulation mode

The tractor exhibits three typical working modes: transport mode, plowing mode, and rotary plowing mode, each corresponding to different operational requirements. The transport and plowing modes are categorized as large-load dragging operations, where only the drive wheel outputs power. Therefore, in the optimization calculation, the focus is placed on considering the rotary plowing and transport modes.

4.1.1 Transport mode

In the transport mode, the power output from the PTO shaft is not required. Accordingly, the discussion primarily revolves around the torque-speed relationship of the drive shaft. When the power demand of the tractor is minimal, with the drive motor operating independently and synchronizers 1 and 2 disengaged, power is transmitted from the main motor to the drive shaft. The gear ring is locked and subsequently transfers power to the wheels through the main gearbox. The speed and torque relationship can be

mathematically expressed using the lever method and graph theory as follows[51]:

$$\begin{cases} n_b = \dfrac{1}{(1+k)i_a} n_q \\ T_b = -(1+k) i_a T_q \end{cases} \tag{14}$$

where, n_q is the output speed of the drive motor, r/min; n_b is the output speed to the half shaft, r/min; T_q indicates the output torque of the drive motor, N·m; T_b is the output torque to the half shaft, N·m; k is the characteristic parameter of the planetary wheel system; and i_a is the main reduction gear ratio.

When the power demand of the tractor exceeds the high-efficiency range of the drive motor, the PTO motor is engaged to assist in driving. During this operation, the drive and PTO motors work in conjunction, with synchronizers 1 and 2 engaged to the right. The PTO motor's toothed ring brake is locked, allowing power to be transmitted through the meshing gears to the intermediate shaft. The power is further transmitted to the toothed ring of the drive shaft, ultimately being outputted through the planetary carrier. The torque-speed relationship can be mathematically expressed as follows:

$$\begin{cases} n_b = \dfrac{1}{(1+k)i_a} n_q + \dfrac{k}{(1+k)i_{56}i_{78}i_a} n_{\mathrm{p}} \\ T_b = (1+k) i_a T_q = \dfrac{(1+k)i_{56}i_{78}i_a}{k} T_p \end{cases} \tag{15}$$

where, n_p is the PTO motor output speed, r/min; i_{56} is the PTO motor input shaft to intermediate shaft ratio, r/min; i_{78} is the intermediate shaft to drive shaft gear ring ratio, r/min; and i_a is the PTO motor output torque, N·m.

In the transport mode, the vertical load on the tractor's drive wheel is set to 3000 kN, while the maximum static friction in the lateral direction is 3500 kN. A fixed resistance is applied to the tractor model, with a rotary damper added to the drive shaft with a value of 200 N·m. During the simulation, the tractor experiences a constant load and undergoes acceleration from 0 to 20 km/h. The power from the PTO motor passes through Z5/Z6 and Z7/Z8 throughout this process, coupling with the drive motor power transmitted to the drive shaft.

4.1.2 Rotary plowing mode

When the electric tractor is equipped with a farm implement, such as a rototiller, the power output is primarily raised by the PTO axial farm implement, while the driving force is increased by the drive shaft. The drive and PTO motors simultaneously work, allowing the dual motor power distribution and synchronization to be adjusted based on the power requirements of the transmission system.

In the rotary plowing mode, a fixed load is applied to the PTO shaft to simplify the computational complexity of the simulation. Considering the high-density random load spectrum characteristic of the tractor's PTO shaft during the implementation, random loads are introduced on top of the fixed loads applied in the previous section for the transportation mode. This simulation approach aims to emulate real-life rotary plowing working conditions. The team's previous research on the construction of a tractor random load module is utilized to obtain a PTO random load module that is suitable for tractor rotary tillage operations[7,52].

The fixed loads obtained from the transportation mode and the established random load module were combined to simulate the loads on the PTO shafts within the simulation environment. This combined load was then utilized as the output of the variable damper using the Sum module in Simulink. The PTO shaft inertia was set to 50 kg·m^2. The setup of the electric tractor driveline was primarily based on the transportation mode, with the traction resistance adjusted to ensure sufficient power for operation in the rotary plowing mode.

4.2 Hardware-in-the-loop (HIL) simulation

HIL systems are a valuable technique for substituting real systems or specific components with simulation models. In the context of total vehicle control, HIL systems are commonly utilized to test and evaluate authentic machine controllers, where the controlled vehicle and other components are virtualized. Furthermore, a portion of the simulation model can be replaced with an actual vehicle component, which can be connected to the test controller for HIL testing. The HIL system can furnish all the necessary simulation signals by adhering to the communication requirements.

The HIL system is composed of two primary components: hardware and software. This system can be further categorized into four relatively independent subsystems: the HIL platform, high-speed data transmission system, host computer, and controller (Figure 11).

In the architecture depicted in Figure 11, the HIL platform of the electric tractor is loaded with simulation conditions for transportation and tillage operations. The controller incorporates the DDPG algorithm, enabling in-loop testing of the electric tractor's control hardware. This setup facilitates the dynamic joint simulation of the dynamic optimization model for transmission system parameters and the overall machine model. Figure 12 provides a visual representation of this setup.

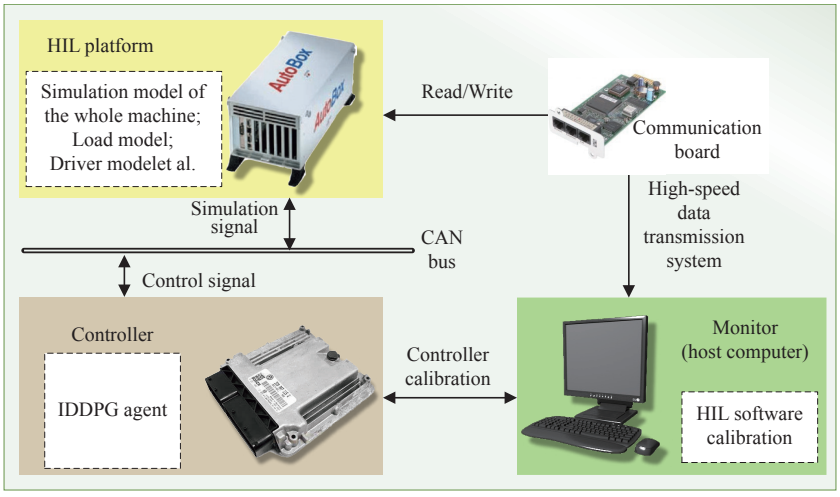

Figure 11 System architecture for HIL testing

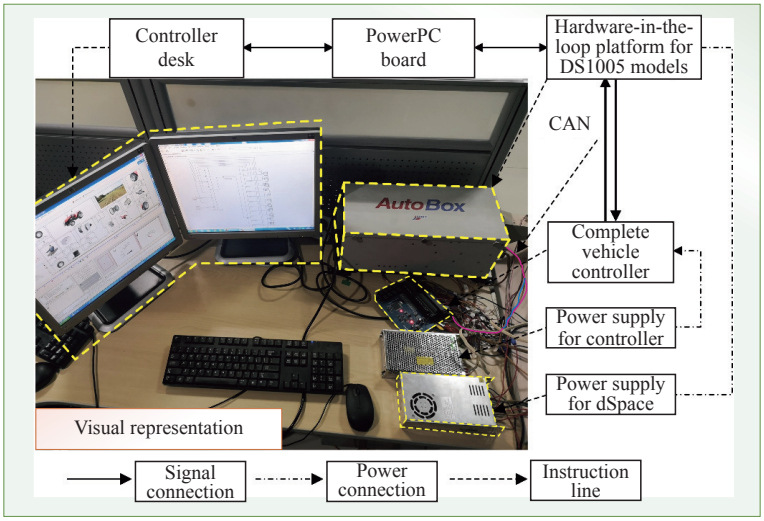

Figure 12 HIL simulation system schematic for electric tractors

The objectives of the HIL simulation are established to attain a vehicle speed of 20 km/h in the transport mode and 15 km/h in the plowing mode, starting from a standstill. The control variables considered in this simulation are the gear ratios of Z6 to Z5 and Z8 to Z7 in the transport mode and the gear ratios of Z4 to Z3 and Z2 to Z1 in the rotary plowing mode.

4.3 Analysis of the optimization results

In this section, we compare and analyze the optimized values of gear teeth, motor efficiency, and vehicle speed obtained through the IDDPG algorithm with their respective original values under conventional static design. The number of gear teeth, motor efficiency, and vehicle speed are taken as parameters for evaluation, enabling a comprehensive assessment of the improvements achieved through the IDDPG algorithm.

4.3.1 Analysis of the optimization results of the transport mode

Stable points in the reward function correspond to conditions where motor efficiency is maximized and transmission ratios align with the operational requirements, minimizing energy losses and system shock. The training results of the IDDPG in the transportation mode are depicted in Figure 13. The oscillations observed in the early training stages are due to the exploration-exploitation trade-off in the reinforcement learning process. Convergence is achieved after approximately 150 episodes, indicating the stability of the IDDPG algorithm. The result of the analysis of the transmission ratio of the two pairs of gears indicates that the optimized gear ratios for gears 5 and 6 stabilize at 3.2, while gears 7 and 8 stabilize at 2.5. In the comparison of these optimized ratios with the pre-optimization ratios, we find a reduction of 0.7 in the transmission ratio for the transport mode. The result of the matching of the transmission system parameters indicates that the optimal numbers of teeth for gears 5 and 6 are 30 and 97, while those for gears 7 and 8 are 34 and 81, respectively.

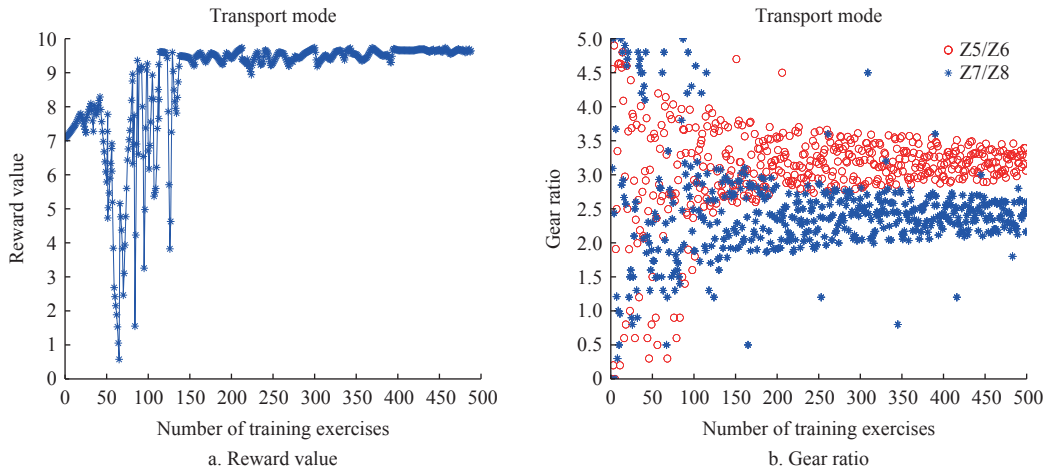

a. Reward value b. Gear ratio

Figure 13 Training results of IDDPG in transportation mode

Figure 14 illustrates the relationship between motor efficiency, tractor speed, and time for the transportation mode under the traditional static design and the optimized design using the IDDPG algorithm. The results reveal that the tractor achieves a 20 km/h speed 0.3 s faster with the IDDPG algorithm compared with the traditional static design. Additionally, the average motor efficiency during the acceleration and steady driving phases is 82% for the traditional static design, whereas it reaches 92% with the optimized IDDPG algorithm, resulting in a 10% improvement in motor efficiency. The analytical results of the motor control law indicate that although the optimized control law is more complex and challenging, the motor operates within a higher efficiency range, minimizing fluctuations in motor efficiency.

4.3.2 Analysis of the optimization results of the rotary plowing mode

The tractor accelerates from a standstill to 15 km/h during the

simulation process. During this time, the tractor's working mode rapidly switches from transportation to rotary plowing modes. In this mode, a portion of the power from the drive motor is transferred to the PTO axis through gears Z1, Z2, Z3, and Z4, enabling the tractor to maintain a uniform speed of 15 km/h. The training results of the IDDPG algorithm in the rotary plowing mode are depicted in Figure 15. The oscillations observed in the early training stages are due to the exploration-exploitation trade-off in the reinforcement learning process. Convergence is achieved after approximately 500 episodes, indicating the stability of the IDDPG algorithm. After 500 simulations, the gear ratio between gear 1 and gear 2 reaches a stable value of 2.6, while the gear ratio between gear 3 and gear 4 stabilizes at 2.2. These simulation results indicate that the optimized transmission ratio in the transport mode is significantly different from the rotary plowing mode, demonstrating the adaptability and effectiveness of the IDDPG algorithm in enhancing transmission system performance for various tractor working conditions. The results of the matching of the transmission system parameters indicate that the optimal numbers of teeth for gears 1 and 2 are 34 and 89, respectively. Meanwhile, the optimal numbers of teeth for gear 3 and gear 4 are 36 and 79, respectively.

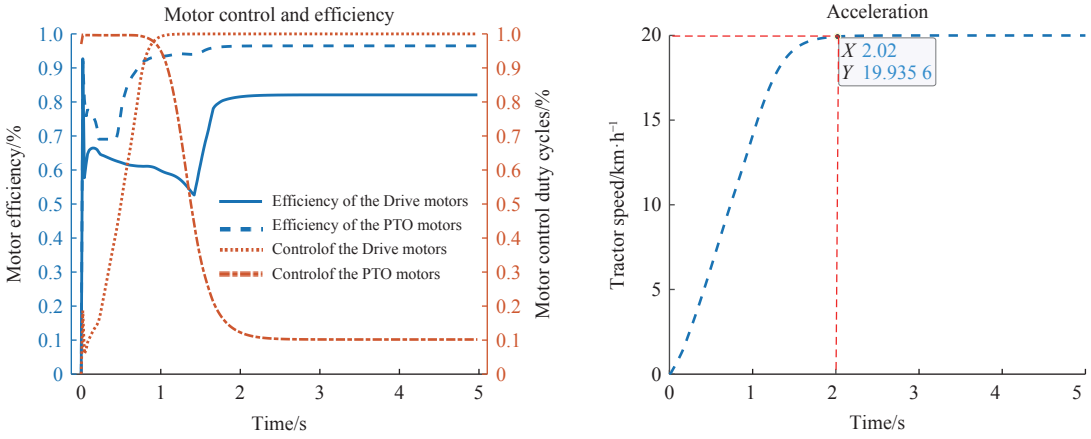

a. Transmission system performance under the traditional static design (Z5/Z6 = 26/93, Z7/Z8 = 31/99)

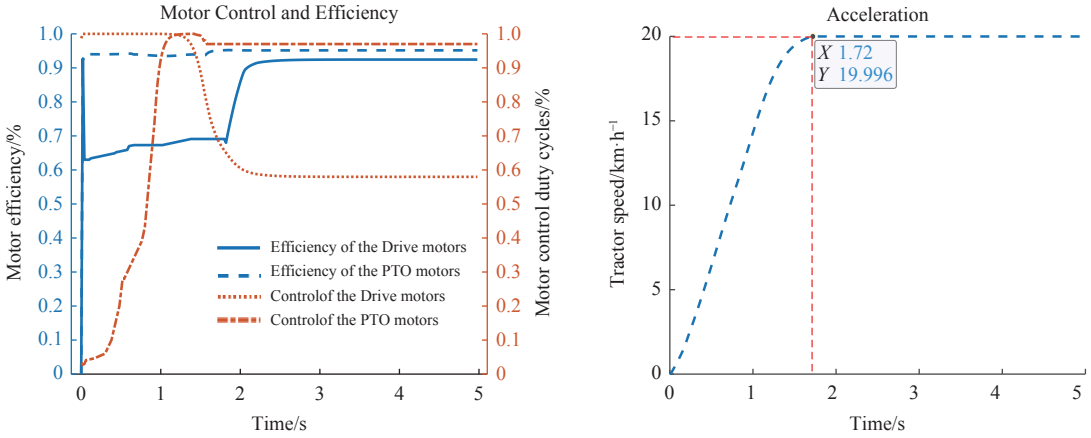

b. Transmission system performance under the IDDPG algorithm (Z5/Z6 = 30/97, Z7/Z8 = 34/81)

Figure 14 Transmission performance of tractors in transport mode

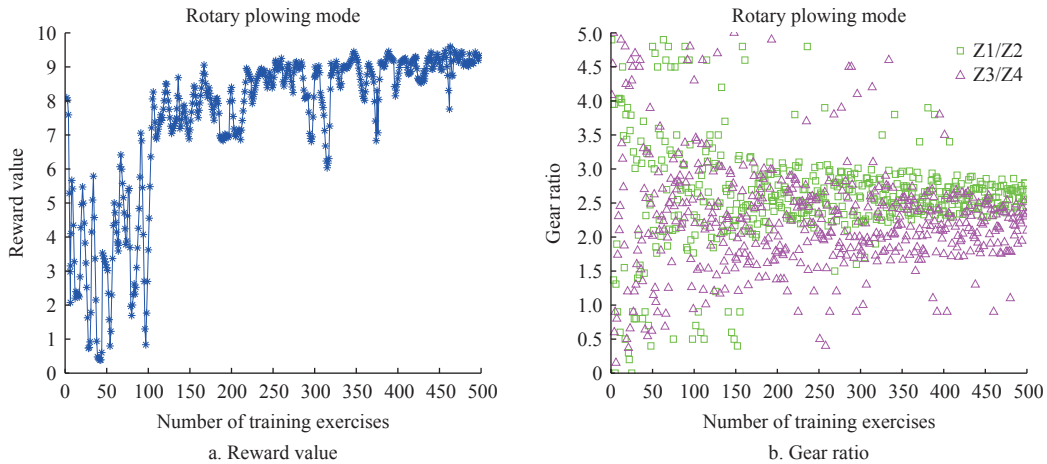

a. Reward value b. Gear ratio

Figure 15 Training results of IDDPG in rotary plowing mode

Figure 16 illustrates the relationship between motor efficiency, tractor speed, and time for rotary plowing under the traditional static design and the optimized design using the IDDPG algorithm. In this analysis, the PTO axle operates in constant speed output mode. The IDDPG algorithm optimized design and the traditional static design both enable the PTO axle to rapidly reach 350 r/min and maintain a stable output. However, the tractor achieves the target speed of 15 km/h in just 2.5 s under the IDDPG algorithm optimized design, while it takes 3.5 s under the traditional static design. This result signifies that the optimized design using the IDDPG algorithm yields a noteworthy improvement in acceleration time, advancing by 1 s compared with the traditional static design. Moreover, the average efficiency of the drive and PTO motors under the optimized design of the IDDPG algorithm reaches 95%, whereas it is 90% under the traditional static design.

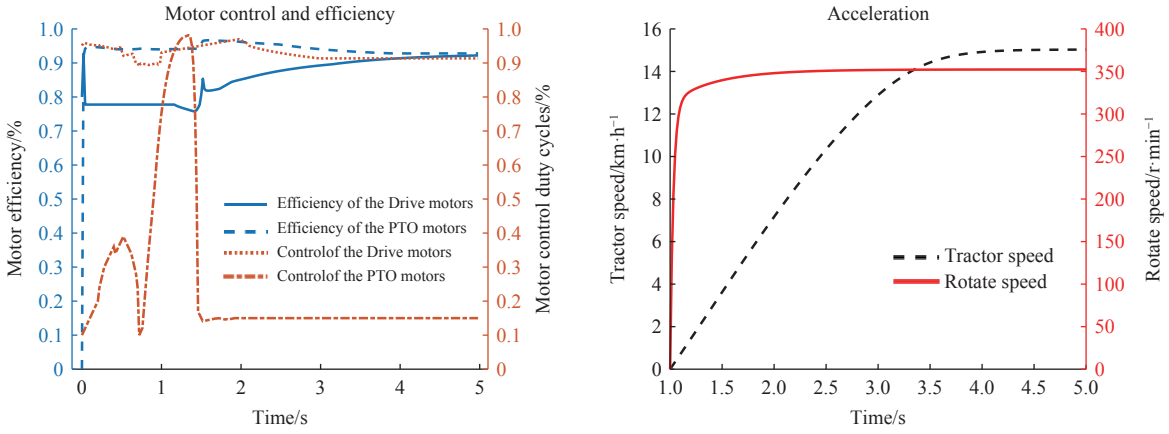

a. Transmission system performance under the traditional static design (Z1/Z2 = 31/99, Z3/Z4 = 29/93)

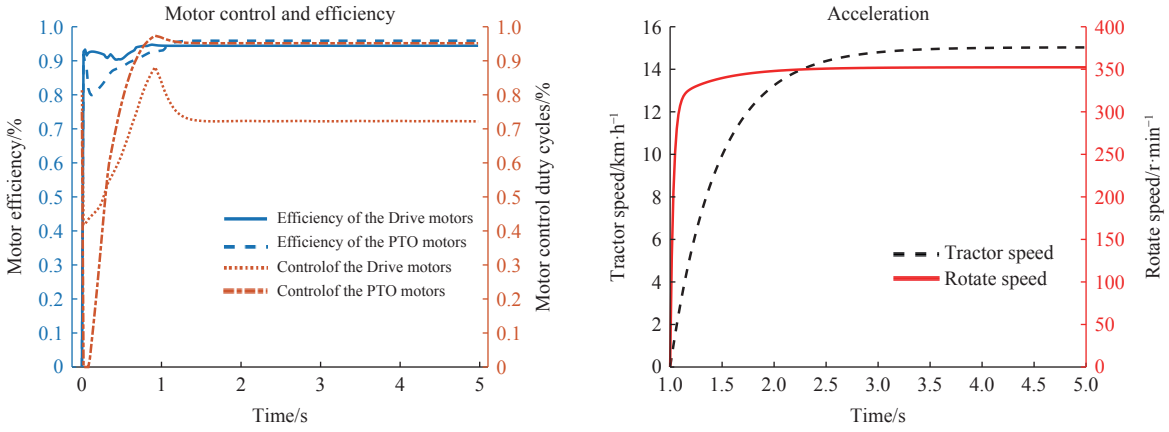

b. Transmission system performance under the IDDPG algorithm (Z1Z2 = 34/89, Z3/Z4 = 36/79)

Figure 16 Transmission performance of tractors in rotary plowing mode

Consequently, the motor efficiency is enhanced by 5% through the use of the IDDPG algorithm, indicating its effectiveness in improving motor performance. An observation of the motor control law reveals that the optimized motor control law is simpler, resulting in reduced control difficulty and a narrower range of motor efficiency fluctuations. Hence, the motor predominantly operates within a higher efficiency interval, further enhancing the system's overall efficiency.

5 Discussion

The operation of an electric tractor transmission system is a complex process, encompassing numerous variables that necessitate consideration in practical engineering. However, our current focus has been directed toward the optimization of a crucial parameter – the ratio of each meshing gear in the transmission – due to computational constraints. Accordingly, the other essential factors, such as gear cost and geometry, have not been included in the current calculation. Enabling these additional parameters to actively participate in the optimization process requires sufficient computing power, which we intend to explore in the forthcoming research articles.

6 Conclusions

This study presents a systematic approach to optimizing the transmission system parameters of dual-motor-driven pure electric tractors, combining advanced reinforcement learning algorithms with virtual prototype technology. By focusing on gear ratio optimization, the study demonstrates significant improvements in the dynamic performance and energy efficiency of electric tractors. The following conclusions can be drawn:

1) We identified a transmission form with dual motor inputs and dual planetary row coupled outputs, enabling power distribution between the drive and the PTO shafts of an electric tractor through the convergence of dual motors. The feasibility of this structure has been demonstrated using conventional static calculations.

2) A virtual prototype environment integrating 3D modeling and Simscape simulation was established, allowing precise performance analysis of the electric tractor's transmission system.

3) An improved IDDPG algorithm successfully addressed fixed coupling limitations, achieving dynamic transmission ratio optimization and enhanced system stability.

4) Finally, we solved for the optimized values of drive train

parameters by altering the electric tractor's working mode, analyzing changes in acceleration performance and motor efficiency under various conditions. Comparative analysis with the traditional static design revealed that the transmission ratio in the transport mode decreased by 10.9%, resulting in a 13.6% advancement in the tractor's time from 0 to 20 km/h, with a 10% increase in the overall motor efficiency. In the rotary plowing mode, the transmission ratio decreased by 25%, advancing the tractor from 0 to 15 km/h by 28.5%, while improving the overall motor efficiency by 5%. The PTO performance remained consistent before and after optimization.

This research provides a methodological framework for integrating advanced reinforcement learning algorithms with virtual prototyping for agricultural machinery optimization. The proposed approach not only enhances the dynamic performance and energy efficiency of electric tractors but also contributes to the sustainable development of agricultural systems. Future studies could extend this framework to incorporate additional optimization parameters, such as manufacturing cost, gear geometry, and multi-objective trade-offs, to further improve the practical applicability and robustness of the system.

Acknowledgements

This research was financially supported by the National Key R&D Program of China (2022YFD2001204), the Engineering Research and Development Project of the Ministry of Industry and Information Technology (CEIEC-2022-ZM02-0225), the Jiangsu Province Modern Agricultural Machinery Equipment and Technology Innovation Demonstration Project (NJ2023-27), and the Nanjing Modern Agricultural Machinery Equipment and Technology Innovation Demonstration Project (NJ[2023]03).

[References]

[1] Wang Y C, Zhou Q Y. Evaluation of Development of Agricultural Modernization in Central China. IERI Procedia, 2013; 4: 417–424.

[2] Vogt H H, de Melo R R, Daher S, Schmuelling B, Antunes F L M, dos Santos P A, et al. Electric tractor system for family farming: Increased autonomy and economic feasibility for an energy transition. Journal of Energy Storage, 2021; 40: 102744.

[3] Lovarelli D, Bacenetti J. Exhaust gases emissions from agricultural tractors: State of the art and future perspectives for machinery operators. Biosystems Engineering, 2019; 186: 204–213.

[4] Gorjian S, Ebadi H, Trommsdorff M, Sharon H, Demant M, Schindele S. The advent of modern solar-powered electric agricultural machinery: A solution for sustainable farm operations. Journal of Cleaner Production, 2021; 292: 126030.

[5] Gao H S, Xue J L. Modeling and economic assessment of electric transformation of agricultural tractors fueled with diesel. Sustainable Energy Technologies and Assessments, 2020; 39: 100697.

[6] Chen Y N, Xie B, Mao E R. Electric tractor motor drive control based on FPGA. IFAC-PapersOnLine, 2016; 49(16): 271–276.

[7] Xu W X, Liu M N, Xu L Y, Zhang S. Energy management strategy of hydrogen fuel cell/battery/ultracapacitor hybrid tractor based on efficiency optimization. Applied Sciences, 2023; 13(1): 151.

[8] Tomasikova M, Tropp M, Gajdosik T, Krzywonos L, Brumercik F. Analysis of transport mechatronic system properties. Procedia Engineering, 2017; 192: 881–886.

[9] Xie B, Wang S, Wu X H, Wen C K, Zhang S L, Zhao X Y. Design and hardware-in-the-loop test of a coupled drive system for electric tractor. Biosystems Engineering, 2022; 216: 165–185.

[10] Wen C K, Zhang S L, Xie B, Song Z H, Li T H, Jia F, Han J G. Design and verification innovative approach of dual-motor power coupling drive systems for electric tractors. Energy, 2022; 247: 123538.

[11] Hu J J, Zu G Q, Jia M X, Niu X Y. Parameter matching and optimal energy management for a novel dual-motor multi-modes powertrain system. Mechanical Systems and Signal Processing, 2019; 116: 113–128.

[12] Zhang S, Xiong R, Zhang C N, Sun F C. An optimal structure selection and parameter design approach for a dual-motor-driven system used in an electric bus. Energy, 2016; 96: 437–448.

[13] Hajduga A. The torque distribution analysis for dual motor - single shaft electric drive. 23rd International Conference on Methods & Models in Automation & Robotics (MMAR), Miedzyzdroje, Poland, 2018; pp.622–627, doi: 10.1109/MMAR.2018.8486022

[14] Hajduga A. Dual motor single shaft powertrain concept. 23rd International Conference on Methods & Models in Automation & Robotics (MMAR), Miedzyzdroje, Poland, 2018; pp.843–848, doi: 10.1109/MMAR.2018.8485871

[15] Moinfar A, Shahgholi G, Gilandeh Y A, Gundoshmian T M. The effect of the tractor driving system on its performance and fuel consumption. Energy, 2020; 202: 117803.

[16] Zhang S L, Ren W, Xie B, Luo Z H, Wen C K, Chen Z J, et al. A combined control method of traction and ballast for an electric tractor in ploughing based on load transfer. Computers and Electronics in Agriculture, 2023; 207: 107750.

[17] Saetti M, Mattetti M, Varani M, Lenzini N, Molari G. On the power demands of accessories on an agricultural tractor. Biosystems Engineering, 2021; 206: 109–122.

[18] Xue L J, Jiang H H, Zhao Y H, Wang J B, Wang G M, Xiao M H. Fault diagnosis of wet clutch control system of tractor hydrostatic power split continuously variable transmission. Computers and Electronics in Agriculture, 2022; 194: 106778.

[19] Wang S, Wu X H, Zhao X Y, Wang S L, Xie B, Song Z H, et al. Co-optimization energy management strategy for a novel dual-motor drive system of electric tractor considering efficiency and stability. Energy, 2023; 281: 128074.

[20] Regazzi N, Maraldi M, Molari G. A theoretical study of the parameters affecting the power delivery efficiency of an agricultural tractor. Biosystems Engineering, 2019; 186: 214–227.

[21] Xia Y, Sun D Y, Qin D T, Zhou X Y. Optimisation of the power-cycle hydro-mechanical parameters in a continuously variable transmission designed for agricultural tractors. Biosystems Engineering, 2020; 193: 12–24.

[22] Chen Y N, Xie B, Du Y F, Mao E R. Powertrain parameter matching and optimal design of dual-motor driven electric tractor. Int J Agric & Biol Eng, 2019; 12(1): 33–41.

[23] Li B G, Sun D Y, Hu M H, Liu J L. Automatic starting control of tractor with a novel powershift transmission. Mechanism and Machine Theory, 2019; 131: 75–91.

[24] Molari G, Sedoni E. Experimental evaluation of power losses in a powershift agricultural tractor transmission. Biosystems Engineering, 2008; 100(2): 177–183.

[25] Choi C, Ahn H, Yu J, Han J-S, Kim S-C, Park Y-J. Optimization of gear macro-geometry for reducing gear whine noise in agricultural tractor transmission. Computers and Electronics in Agriculture, 2021; 188: 106358.

[26] Ouyang T C, Lu Y C, Li S Y, Yang R, Xu P H, Chen N. An improved smooth shift strategy for clutch mechanism of heavy tractor semi-trailer automatic transmission. Control Engineering Practice, 2022; 121: 105040.

[27] Nguyen T, Kriesten R, Chrenko D. Concept for generating energy demand in electric vehicles with a model based approach. Appl. Sci., 2022; 12: 3968.

[28] Mattetti M, Michielan E, Mantovani G, Varani M. Objective evaluation of gearshift process of agricultural tractors. Biosystems Engineering, 2022; 224: 324–335.

[29] Robinette D, Wehrwein D. Automatic transmission gear ratio optimization and monte carlo simulation of fuel consumption with parasitic loss uncertainty. SAE Int. J. Commer. Veh., 2015; 8(1): 45–62.

[30] Tan S Q, Yang J, Zhao X X, Hai T T, Zhang W M. Gear ratio optimization of a multi-speed transmission for electric dump truck operating on the structure route. Energies, 2018; 11(6): 1324.

[31] Spanoudakis P, Moschopoulos G, Stefanoulis T, Sarantinoudis N, Papadokokolakis E, Ioannou I, et al. Efficient gear ratio selection of a single-speed drivetrain for improved electric vehicle energy consumption, Sustainability, 2020;12(21): doi: 10.3390/su12219254.

[32] Eckert J J, Santiciolli F M, Silva L C A, Dedini F G. Vehicle drivetrain design multi-objective optimization. Mech. Mach. Theory, 2021; 156(1): 104123

[33] Li B G, Pan J B, Li Y H, Ni K, Huang W Y, Jiang H J, et al. Optimization method of speed ratio for powershift transmission of agricultural tractor. Machines, 2023; 11: 438.
[34] Neto L S, Jasper S P, Kmiecik L L, Silva T X D, Savi D. Performance of agricultural tractor with and without automatic transmission and engine rotation management. Braz. J. Agric. Environ. Eng., 2021; 25: 498–502.
[35] Oh K, Yun S, Ko K, Ha S, Kim P, Seo J, Yi K. Gear ratio and shift schedule optimization of wheel loader transmission for performance and energy efficiency. Automation in Construction, 2016; 69: 89–101.
[36] Eckert J J, da Silva S F, Santiciolli F M, de Carvalho Á C, Dedini F G. Multi-speed gearbox design and shifting control optimization to minimize fuel consumption, exhaust emissions and drivetrain mechanical losses. Mechanism and Machine Theory, 2022; 169: 104644.
[37] Kramberger J, Šraml M, Glodež S, Flašker J, Potrč I. Computational model for the analysis of bending fatigue in gears. Computers & Structures, 2004; 82(23): 2261–2269.
[38] Bonori G, Barbieri M, Pellicano F. Optimum profile modifications of spur gears by means of genetic algorithms. Journal of Sound and Vibration, 2008; 313(3): 603–616.
[39] Pedrero J I, Pleguezuelos M, Sánchez M B. Study of the influence of the design parameters on the efficiency of spur gears. In P. Velex (Ed.), International Gear Conference 2014, August 26th–28th, Lyon, Oxford: Chandos Publishing, 2014; pp.774–783.
[40] Yuan B, Chang S, Liu G, Chang L H, Liu L. Quasi-static analysis based on generalized loaded static transmission error and dynamic investigation of wide-faced cylindrical geared rotor systems. Mechanism and Machine Theory, 2019; 134: 74–94.
[41] Pawar P B, Utpat A A. Analysis of composite material spur gear under static loading condition. materials today: Proceedings, 2015; 2(4): 2968–2974.
[42] Martin T C, Orchard M E, Sánchez P V. Design and simulation of control strategies for trajectory tracking in an autonomous ground vehicle. IFAC Proceedings Volumes, 2013; 46(24): 118–123.
[43] Joa E, Cha H, Hyun Y, Koh Y, Yi K, Park J. A new control approach for automated drifting in consideration of the driving characteristics of an expert human driver. Control Engineering Practice, 2020; 96: 104293.
[44] Guo W F, Zhao S, Cao H T, Yi B L, Song X L. Koopman operator-based driver-vehicle dynamic model for shared control systems. Applied Mathematical Modelling, 2023; 114: 423–446.
[45] Takeda M, Inoue M, Fang X, Minami Y, Maestre J M. Light guidance control of human drivers: driver modeling, control system design, and VR experiment. IFAC-PapersOnLine, 2022; 55(41): 32–37.
[46] Winkler N, Drugge L, Trigell A S, Efraimsson G. Coupling aerodynamics to vehicle dynamics in transient crosswinds including a driver model. Computers & Fluids, 2016; 138: 26–34.
[47] Li X Z, Liu M N, Xu L Y, Zhang M Z, Yan X H. Design and test of tractor serial hydraulic and mechanical hybrid transmission system. Transactions of the CSAM, 2022; 53(1): 406–413.
[48] Zhang J, Chen D, Wang S M, Hu X A, Wang D. Deign and experiment of four-wheel independent steering driving and control system for agricultural wheeled robot. Transactions of the CSAE, 2015; 31(18): 63–70.
[49] Liu M, Wei C, Xu L. Development of cooperative controller for dual-motor independent drive electric tractor. Mathematical Problems in Engineering, 2020; 2020: 1–12.
[50] Lillicrap T P, Hunt J J, Pritzel A, Heess N, Erez T, Tassa Y, et al. Continuous control with deep reinforcement learning. Computer Science, 2019; arXiv: 1509.02971. doi: arxiv.org/abs/1509.02971v6
[51] Xu L, Zhou Z, Zhang M, Li Y. Design of hydro—mechanical continuously variable transmission of tractor. Transactions of the CSAM, 2006; 37(7): 5–8.
[52] Liu M N, Zhou Z L, Xu L Y, Zhao J H, Meng T. Electric tractor energy system and management strategy research based on load power spectral density. Transactions of the CSAM, 2018; 49(2): 358–366.